Supplement of Biogeosciences, 16, 1343–1360, 2019
https://doi.org/10.5194/bg-16-1343-2019-supplement

Biogeosciences Open Access EGU

Supplement of

Plant responses to volcanically elevated CO_2 in two Costa Rican forests

Robert R. Bogue et al.

Correspondence to: Florian M. Schwandner (florian.schwandner@jpl.caltech.edu)

Supplementary Info

We analyzed how CO_2 emissions vary spatially along radial transects across a sample of volcanoes from around the world. We used published data from a variety of volcanoes, either in the form of individual point measurements or spatially simulated flux maps. Because magnitude of CO_2 emissions varies significantly between volcanoes, we took the $\log_{10}$ of the flux or concentration values and then transformed these values into a relative scale from 0 to 1, where 1 was the maximum flux or concentration at a specific volcano. For some groups of transects that had similar magnitudes of CO_2 emissions they were all put on the same relative scale. All CO_2 data was then linearly detrended. The distance along the radial transect was also put into a relative scale from 0 to 1, where 0 was the beginning of the transect and 1 was the end of the transect. The volcanoes and publications we took data from are as follows: Arenal (Williams-Jones, 1997), Teide (Hernández et al., 1998), Furnas (Viveiros et al., 2010), Vesuvius (Frondini et al., 2004), Vulcano (Schwandner et al., 2004), Cerro Negro (Salazar et al., 2001), Etna (Allard et al., 1991), Irazú (our collected data), and Mammoth Mountain (Werner et al., 2014). The data plotted in the supplemental Figure 1 show that all volcanoes studied show significant variations in volcanic CO_2 flux across their flanks, likely due to varying permeability (substrate) and fracture-controlled advective transport of CO_2 feeding these emissions from depth. These variations allow to study volcanically enhanced levels of CO_2 emissions as proxies for future atmospheric conditions via two modes: a local, substrate- and altitude-independent mode on the order of 50-200 meters, and a broad-scale enhancement mode, covering much of the volcanic flanks (distances on the order of 5-20 km) at lower levels of enhancements.

To validate the understanding that CO_2 in sub-canopy air is highly variable and not well mixed, while eCO_2 flux through the soil to the atmosphere is highly stable, we assessed the differences in variability between instantaneous concentrations in sub-canopy air and that inside the measurement chamber. The CO_2 concentration in air were collected at approx. 0.2 m and 2.0 m above ground level, before and after flux measurements were performed. Supplemental figure 2 shows a sample of near-simultaneous CO_2 concentrations recorded on March 24, 2017 at ground level (0.2 m agl) and at 2 m above ground, at a site near the Arieta Fault, in unmanaged forest ~1.3 km southwest of Turrialba's central crater, a site of known high eCO_2 flux (Epiard et al., 2017). CO_2 concentrations inside the measurement chamber during soil-to-atmosphere eCO_2 flux measurements show continuous and highly stable addition of eCO_2 to the chamber air from below. The measurements in the sub-canopy air consistently showed very high variability. For instantaneous survey measurements of eCO_2 over a range of sites, long-term averaging and flux modeling to assess in-canopy exposure enhancements is not feasible. In contrast, emission of eCO_2 through the soil can be quickly and stably assessed in surveys using in-situ chamber flux measurements. The excess component (relative to the regional background) that is closer to the ground likely represents a stronger volcanic eCO_2 portion from the direct area of emission measured on the ground, than the excess component shown in the 2 m above ground data, which show stronger temporary deviations. Because absolute mean eCO_2 exposures at canopy level are hard to assess, we utilize the highly stable emission rates of volcanic eCO_2 through the soil as a relative proxy for long-time eCO_2 exposure differences between sites.

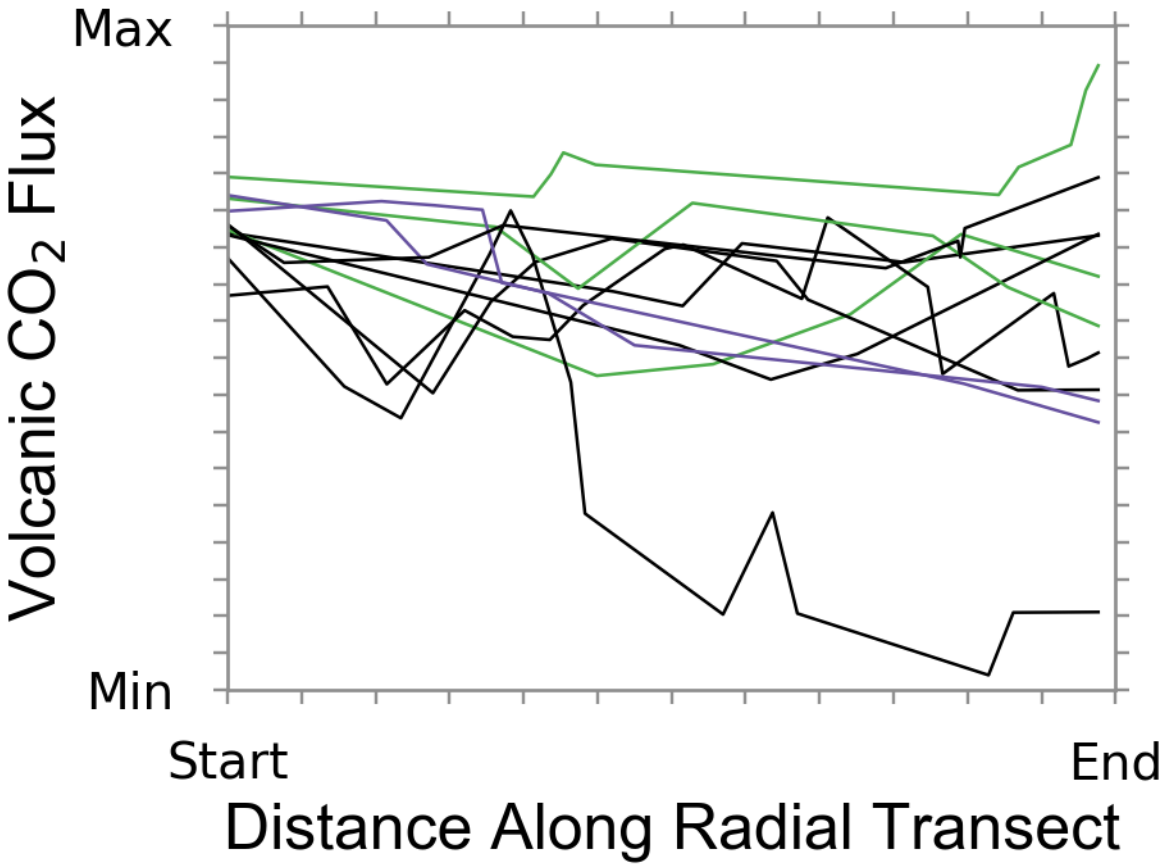

Fig. S1: CO_2 flux varies significantly along radial transects from 11 volcanoes around the world.

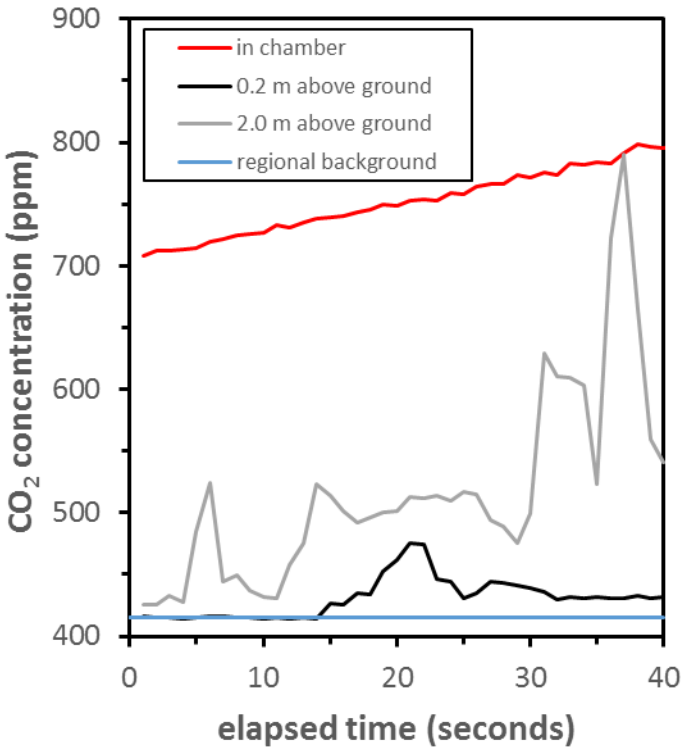

Fig. S2: CO_2 concentrations and fluxes in sub-canopy air are highly variable, while soil-to-atmosphere eCO_2 fluxes are stable representations of long-term eCO_2 addition (March 24, 2017, in a forest near the Ariete fault on Turrialba volcano).

Species	Latitude	Longitude	Max CO_2 flux ($g\ m^{-2}\ day^{-1}$)	Mean CO_2 flux ($g\ m^{-2}\ day^{-1}$)	CO_2 flux 1σ	$\delta^{13}C$ (‰)	CCI	CCI 1σ	Chlorophyll concentration (umol m^-2)	Chlorophyll concentration 1σ	Fv/Fm	Fv/Fm 1σ	g_s	g_s 1σ
A. acuminata	10° 0'14.42"N	83°46'7.31"W	7.1	6.1	0.7	-26.1	28.7	8.6	452.4	135.5	0.793	0.017	83.5	7.8
A. acuminata	10° 0'17.87"N	83°46'9.20"W	18.5	11.1	6.6	-26.58	32.3	2.7	485.6	41.1	0.812	0.013	153.5	9.2
A. acuminata	10° 0'18.52"N	83°46'7.11"W	6.5	4.1	2.5	-24.48	25.7	8.0	423.5	132.7	0.793	0.011		
A. acuminata	10° 0'17.69"N	83°46'8.72"W	18.5	11.1	6.6	-26.22	33.0	4.7	491.8	70.0	0.806	0.013	241.0	79.2
A. acuminata	9°59'52.79"N	83°46'13.90"W	8.8	8.0	0.8	-25.76	20.8	5.6	371.9	100.7	0.801	0.010	131.5	17.7
A. acuminata	9°59'52.45"N	83°46'14.53"W	13.0	10.6	2.3	-26.24	40.7	6.7	556.1	91.5	0.824	0.005	331.5	51.6
B. nitida	9°58'60.00"N	83°50'9.15"W	15.7	9.6	4.2		56.1	29.6	669.4	352.8	0.838	0.018		
B. nitida	9°59'16.85"N	83°50'26.77"W	18.1	16.8	1.8		11.9	0.1	259.6	2.5	0.805	0.009		
B. nitida	10° 0'41.38"N	83°50'4.43"W	43.4	37.5	8.4		44.0	1.9	582.0	24.8	0.832	0.004		
B. nitida	10° 0'14.38"N	83°46'6.65"W	18.7	13.2	5.1	-26.76	83.1	1.4	834.6	14.5	0.799	0.009		
B. nitida	10° 0'18.54"N	83°46'7.15"W	6.5	4.1	2.5	-28.12	35.2	12.3	510.9	178.5	0.823	0.009		
B. nitida	10° 0'15.89"N	83°46'10.65"W	31.5	25.0	5.9	-26.22	80.3	1.9	819.0	19.4	0.795	0.012	160.0	0.0
B. nitida	9°59'56.46"N	83°46'31.92"W	5.7	4.6	1.1	-27.5	86.4	15.9	852.7	156.6	0.840	0.012	171.3	48.9
B. nitida	9°59'57.83"N	83°46'33.99"W	19.7	15.7	9.9	-26.72	99.5	15.3	921.9	141.5	0.840	0.012	200.5	14.8
B. nitida	9°59'55.11"N	83°46'36.36"W	21.5	15.6	7.9	-27.46	65.7	15.1	731.8	167.8	0.830	0.009	199.5	38.9
O. xalapensis	9°58'60.00"N	83°50'9.15"W	15.7	9.6	4.2		25.7	2.1	424.0	34.2	0.804	0.007		
O. xalapensis	10° 0'11.84"N	83°49'39.52"W	9.3	9.3	4.7		31.9	0.9	482.0	14.1	0.888	0.038		
O. xalapensis	10° 0'20.32"N	83°46'7.94"W	8.8	6.2	3.7	-26.31	22.7	2.0	393.2	35.3	0.783	0.016	190.0	0.0
O. xalapensis	9°59'56.41"N	83°46'12.18"W	12.2	5.7	4.5	-26.58	29.3	12.2	458.5	191.2	0.784	0.024	232.5	99.7
O. xalapensis	9°59'51.80"N	83°46'14.70"W	24.2	10.6	11.8	-25.51	39.4	5.2	546.1	72.2	0.806	0.010	321.0	45.3
O. xalapensis	9°59'52.21"N	83°46'12.76"W	10.0	7.0	3.0	-26.03	59.6	15.9	692.3	185.1	0.807	0.001	267.0	97.6
O. xalapensis	9°59'50.79"N	83°46'12.73"W	5.5	4.0	1.7	-27.16	66.5	13.9	736.8	153.5	0.804	0.012	306.0	59.4
O. xalapensis	9°59'56.47"N	83°46'31.92"W	5.7	4.6	1.1	-26.46	67.0	14.5	740.1	160.4	0.801	0.013	330.5	20.5

Table S1: Data used to generate all plots.

Species	Latitude	Longitude	Altitude (m)	Pressure (mbars)	Humidity (%)	PAR (μmol m^{-2} s^{-1})	Air T (°C)	Leaf T (°C)	Wind (m/s)	Aspect (degrees)	Slope (degrees)	DBH (cm)
A. acuminata	10° 0'14.42"N	83°46'7.31"W	2638	734.4	64	198	15.8	16	0	270	5	24.9
A. acuminata	10° 0'17.87"N	83°46'9.20"W	2640		70.55	150	12.5	13			0	14.3
A. acuminata	10° 0'18.52"N	83°46'7.11"W	2636	734.6	77.1	110	13.7	14.1	0	215	60	23
A. acuminata	10° 0'17.69"N	83°46'8.72"W	2633	734.8	84.5	173	15.5	15.4	0	290	5	45.3
A. acuminata	9°59'52.79"N	83°46'13.90"W	2432		64.9	200	15	15.4		135	25	58
A. acuminata	9°59'52.45"N	83°46'14.53"W	2434		65.2	325	15.4	15.5		110	20	90.3
B. nitida	9°58'60.00"N	83°50'9.15"W	3016	700	86.5	363	10.8	11.3	0	140	45	22.7
B. nitida	9°59'16.85"N	83°50'26.77"W	2968			94	12	11.2		20	50	50.2
B. nitida	10° 0'41.38"N	83°50'4.43"W	2322	763.7	84.4	86	12.9	13.4	0.5	120	55	43.5
B. nitida	10° 0'14.38"N	83°46'6.65"W	2619	735.9	67.6	800	12.6	13.4	1.7	190	35	15.3
B. nitida	10° 0'18.54"N	83°46'7.15"W	2615	736.4	89.5	172	13.4	12.9	0.4	215	60	11.5
B. nitida	10° 0'15.89"N	83°46'10.65"W	2625		85.7	334	13.6	13.8	1	200	15	26
B. nitida	9°59'56.46"N	83°46'31.92"W	2515	745.8	49.3	128	13.7	14	0	250	25	190
B. nitida	9°59'57.83"N	83°46'33.99"W	2511	746.2	67.7	157	13.9	13.9	0.2	180	5	180
B. nitida	9°59'55.11"N	83°46'36.36"W	2514	745.9	78.2	98	12.8	12.9	0	125	10	150
O. xalapensis	9°58'60.00"N	83°50'9.15"W	3016	700	86.5	43	10.4	10	0	45	58	15
O. xalapensis	10° 0'11.84"N	83°49'39.52"W	2101	785.4	100	37	15.4	15.2	0	80	30	11
O. xalapensis	10° 0'20.32"N	83°46'7.94"W	2619	736.1	77.9	170	13.5		0	150	55	15.4
O. xalapensis	9°59'56.41"N	83°46'12.18"W	2437	753	64.7	29	12	11.8	0	190	15	20.2
O. xalapensis	9°59'51.80"N	83°46'14.70"W	2438		65.5	325	14.7	14.7		190	55	20.3
O. xalapensis	9°59'52.21"N	83°46'12.76"W	2439		65.7	388	15.5	14.9		310	40	25
O. xalapensis	9°59'50.79"N	83°46'12.73"W	2438	752.9	65.8	338	17.7	17.7	0	285	60	22.5
O. xalapensis	9°59'56.47"N	83°46'31.92"W	2515	745.8	49.3	553	13.9	17.4	0	250	25	27.2

Table S2: Supplementary info for data presented in Table S1.

References

Allard, P., Carbonnelle, J., Dajlevic, D., Le Bronec, J., Morel, P., C. Robe, M., M. Maurenas, J., Faivre-Pierret, R., Martin, D., Sabroux, J.-C. and Zettwoog, P.: Eruptive and diffuse emissions of CO_2 from Mount Etna, Nature, 351, 387–391, doi:DOI: 10.1038/351387a0, 1991.

Epiard, M., Avard, G., de Moor, J. M., Martínez Cruz, M., Barrantes Castillo, G. and Bakkar, H.: Relationship between Diffuse CO_2 Degassing and Volcanic Activity. Case Study of the Poás, Irazú, and Turrialba Volcanoes, Costa Rica, Front. Earth Sci., 5, doi:10.3389/feart.2017.00071, 2017.

Frondini, F., Chiodini, G., Caliro, S., Cardellini, C., Granieri, D. and Ventura, G.: Diffuse CO_2 degassing at Vesuvio, Italy, Bull. Volcanol. Heidelb., 66(7), 642–651, doi:http://dx.doi.org/10.1007/s00445-004-0346-x, 2004.

Hernández, P. A., Pérez, N. M., Salazar, J. M., Nakai, S., Notsu, K. and Wakita, H.: Diffuse emission of carbon dioxide, methane, and helium-3 from Teide Volcano, Tenerife, Canary Islands, Geophys. Res. Lett., 25(17), 3311–3314, doi:10.1029/98GL02561, 1998.

Salazar, J. M. L., Hernández, P. A., Pérez, N. M., Melián, G., Álvarez, J., Segura, F. and Notsu, K.: Diffuse emission of carbon dioxide from Cerro Negro Volcano, Nicaragua, Central America, Geophys. Res. Lett., 28(22), 4275–4278, doi:10.1029/2001GL013709, 2001.

Schwandner, F. M., Seward, T. M., Gize, A. P., Hall, P. A. and Dietrich, V. J.: Diffuse emission of organic trace gases from the flank and crater of a quiescent active volcano (Vulcano, Aeolian Islands, Italy), J. Geophys. Res. Atmospheres, 109(D4), D04301, doi:10.1029/2003JD003890, 2004.

Viveiros, F., Cardellini, C., Ferreira, T., Caliro, S., Chiodini, G. and Silva, C.: Soil CO_2 emissions at Furnas volcano, São Miguel Island, Azores archipelago: Volcano monitoring perspectives, geomorphologic studies, and land use planning application, J. Geophys. Res. Solid Earth, 115(B12), B12208, doi:10.1029/2010JB007555, 2010.

Werner, C., Bergfeld, D., Farrar, C. D., Doukas, M. P., Kelly, P. J. and Kern, C.: Decadal-scale variability of diffuse CO_2 emissions and seismicity revealed from long-term monitoring (1995–2013) at Mammoth Mountain, California, USA, J. Volcanol. Geotherm. Res., 289, 51–63, doi:10.1016/j.jvolgeores.2014.10.020, 2014.

Williams-Jones, G.: The Distribution and Origin of Radon, CO_2 and SO_2 Gases at Arenal Volcano, Costa Rica, Université de Montréal., 1997.